EURASIP Journal on Applied Signal Processing 2004:7, 926–933

Physical Modeling of the Piano

N. Giordano
Department of Physics, Purdue University, 525 Northwestern Avenue, West Lafayette, IN 47907-2036, USA
Email: ng@physics.purdue.edu

M. Jiang
Department of Physics, Purdue University, 525 Northwestern Avenue, West Lafayette, IN 47907-2036, USA
Department of Computer Science, Montana State University, Bozeman, MT 59715, USA
Email: jiang@cs.montana.edu

Received 21 June 2003; Revised 27 October 2003

A project aimed at constructing a physical model of the piano is described. Our goal is to calculate the sound produced by the instrument entirely from Newton's laws. The structure of the model is described along with experiments that augment and test the model calculations. The state of the model and what can be learned from it are discussed.

Keywords and phrases: physical modeling, piano.

1. INTRODUCTION

This paper describes a long term project by our group aimed at physical modeling of the piano. The theme of this volume, model based sound synthesis of musical instruments, is quite broad, so it is useful to begin by discussing precisely what we mean by the term "physical modeling." The goal of our project is to use Newton's laws to describe *all* aspects of the piano. We aim to use $F = ma$ to calculate the motion of the hammers, strings, and soundboard, and ultimately the sound that reaches the listener.

Of course, we are not the first group to take such a Newton's law approach to the modeling of a musical instrument. For the piano, there have been such modeling studies of the hammer-string interaction [1, 2, 3, 4, 5, 6, 7, 8, 9], string vibrations [8, 9, 10], and soundboard motion [11]. (Nice reviews of the physics of the piano are given in [12, 13, 14, 15].) There has been similar modeling of portions of other instruments (such as the guitar [16]), and of several other complete instruments, including the xylophone and the timpani [17, 18, 19]. Our work is inspired by and builds on this previous work.

At this point, we should also mention how our work relates to other modeling work, such as the digital waveguide approach, which was recently reviewed in [20]. The digital waveguide method makes extensive use of physics in choosing the structure of the algorithm; that is, in choosing the proper filter(s) and delay lines, connectivity, and so forth, to properly match and mimic the Newton's law equations of motion of the strings, soundboard, and other components of the instrument. However, as far as we can tell, certain features of the model, such as hammer-string impulse functions and the transfer function that ultimately relates the sound pressure to the soundboard motion (and other similar transfer functions), are taken from experiments on real instruments. This approach is a powerful way to produce realistic musical tones efficiently, in real time and in a manner that can be played by a human performer. However, this approach cannot address certain questions. For example, it would not be able to predict the sound that would be produced if a radically new type of soundboard was employed, or if the hammers were covered with a completely different type of material than the conventional felt. The physical modeling method that we describe in this paper can address such questions. Hence, we view the ideas and method embodied in work of Bank and coworkers [20] (and the references therein) as complementary to the physical modeling approach that is the focus of our work.

In this paper, we describe the route that we have taken to assembling a complete physical model of the piano. This complete model is really composed of interacting submodels which deal with (1) the motions of the hammers and strings and their interaction, (2) soundboard vibrations, and (3) sound generation by the vibrating soundboard. For each of these submodels we must consider several issues, including selection and implementation of the computational algorithm, determination of the values of the many parameters that are involved, and testing the submodel. After considering each of the submodels, we then describe how they are combined to produce a complete computational piano. The

quality of the calculated tones is discussed, along with the lessons we have learned from this work. A preliminary and abbreviated report on this project was given in [21].

2. OVERALL STRATEGY AND GOALS

One of the first modeling decisions that arises is the question of whether to work in the frequency domain or the time domain. In many situations, it is simplest and most instructive to work in the frequency domain. For example, an understanding of the distribution of normal mode frequencies, and the nature of the associated eigenvectors for the body vibrations of a violin or a piano soundboard, is very instructive. However, we have chosen to base our modeling in the time domain. We believe that this choice has several advantages. First, the initial excitation—in our case this is the motion of a piano hammer just prior to striking a string—is described most conveniently in the time domain. Second, the interaction between various components of the instrument, such as the strings and soundboard, is somewhat simpler when viewed in the time domain, especially when one considers the early "attack" portion of a tone. Third, our ultimate goal is to calculate the room pressure as a function of time, so it is appealing to start in the time domain with the hammer motion and stay in the time domain throughout the calculation, ending with the pressure as would be received by a listener. Our time domain modeling is based on finite difference calculations [10] that describe all aspects of the instrument.

A second element of strategy involves the determination of the many parameters that are required for describing the piano. Ideally, one would like to determine all of these parameters *independently*, rather than use them as fitting parameters when comparing the modeling results to real (measured) tones. This is indeed possible for *all* of the parameters. For example, dimensional parameters such as the string diameters and lengths, soundboard dimensions, and bridge positions, can all be measured from a real piano. Likewise, various material properties such as the string stiffness, the elastic moduli of the soundboard, and the acoustical properties of the room in which the numerical piano is located, are well known from very straightforward measurements. For a few quantities, most notably the force-compression characteristics of the piano hammers, it is necessary to use separate (and independent) experiments.

This brings us to a third element of our modeling strategy—the problem of how to test the calculations. The final output is the sound at the listener, so one could "test" the model by simply evaluating the sounds via listening tests. However, it is very useful to separately test the submodels. For example, the portion of the model that deals with soundboard vibrations can be tested by comparing its predictions for the acoustic impedance with direct measurements [11, 22, 23, 24]. Likewise, the room-soundboard computation can be compared with studies of sound production by a harmonically driven soundboard [25]. This approach, involving tests against specially designed experiments, has proven to be extremely valuable.

The issue of listening tests brings us to the question of goals, that is, what do we hope to accomplish with such a modeling project? At one level, we would hope that the calculated piano tones are realistic and convincing. The model could then be used to explore what various hypothetical pianos would sound like. For example, one could imagine constructing a piano with a carbon fiber soundboard, and it would be very useful to be able to predict its sound ahead of time, or to use the model in the design of the new soundboard. On a different and more philosophical level, one might want to ask questions such as "what are the most important elements involved in making a piano sound like a piano?" We emphasize that it is *not* our goal to make a real time model, nor do we wish to compete with the tones produced by other modeling methods, such as sampling synthesis and digital waveguide modeling [20].

3. STRINGS AND HAMMERS

Our model begins with a piano hammer moving freely with a speed v_h just prior to making contact with a string (or strings, since most notes involve more than one string). Hence, we ignore the mechanics of the action. This mechanics is, of course, quite important from a player's perspective, since it determines the touch and feel of the instrument [26]. Nevertheless, we will ignore these issues, since (at least to a first approximation) they are not directly relevant to the composition of a piano tone and we simply take v_h as an input parameter. Typical values are in the range 1–4 m/s [9].

When a hammer strikes a string, there is an interaction force that is a function of the compression of the hammer felt, y_f. This force determines the initial excitation and is thus a crucial factor in the composition of the resulting tone. Considerable effort has been devoted to understanding the hammer-string force [1, 2, 3, 4, 5, 6, 7, 27, 28, 29, 30, 31, 32, 33]. Hammer felt is a very complicated material [34], and there is no "first principles" expression for the hammer-string force relation $F_h(y_f)$. Much work has assumed a simple power law function

$$F_h(y_f) = F_0 y_f^p, \tag{1}$$

where the exponent p is typically in the range 2.5–4 and F_0 is an overall amplitude. This power law form seems to be at least qualitatively consistent with many experiments and we therefore used (1) in our initial modeling calculations.

While (1) has been widely used to analyze and interpret experiments, and also in previous modeling work, it has been known for some time that the force-compression characteristic of most real piano hammers is not a simple reversible function [7, 27, 28, 29, 30]. Ignoring the hysteresis has seemed reasonable, since the magnitude of the irreversibility is often found to be small. Figure 1 shows the force-compression characteristic for a particular hammer (a Steinway hammer from the note middle C) measured in two different ways. In the type I measurement, the hammer struck a stationary force sensor and the resulting force and felt compression were measured as described in [31]. We see

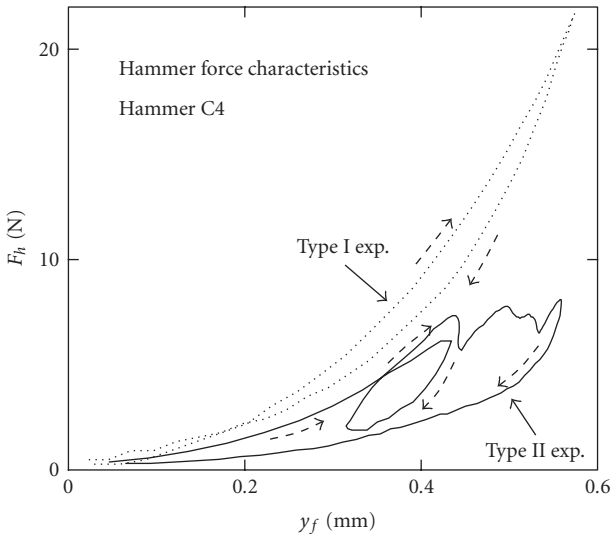

Figure 1: Force-compression characteristics measured for a particular piano hammer measured in two different ways. In the type I experiment (dotted curve), the hammer struck a stationary force sensor and the resulting force, F_h, and felt compression, y_f, were measured. The initial hammer velocity was approximately 1 m/s. The solid curve is the measured force-compression relation obtained in a type II measurement, in which the same hammer impacted a piano string. This behavior is described qualitatively by (2), with parameters $p = 3.5$, $F_0 = 1.0 \times 10^{13}$ N, $\epsilon_0 = 0.90$, and $\tau_0 = 1.0 \times 10^{-5}$ second. The dashed arrows indicate compression/decompression branches.

that for a particular value of the felt compression, y_f, the force is larger during the compression phase of the hammer-string collision than during decompression. However, this difference is relatively small, generally no more than 10% of the total force. Provided that this hysteresis is ignored, the type I result is described reasonably well by the power law function (1) with $p \approx 3$. However, we will see below that (1) is *not* adequate for our modeling work, and this has led us to consider other forms for F_h.

In order to shed more light on the hammer-string force, we developed a new experimental approach, which we refer to as a type II experiment, in which the force and felt compression are measured as the hammer impacts on a string [32, 35]. Since the string rebounds in response to the hammer, the hammer-string contact time in this case is considerably longer (by a factor of approximately 3) than in the type I measurement. The force-compression relation found in this type II measurement is also shown in Figure 1. In contrast to the type I measurements, the type II results for $F_h(y)$ do not consist of two simple branches (one for compression and another for decompression). Instead, the type II result exhibits "loops," which arise for the following reason. When the hammer first contacts the string, it excites pulses that travel to the ends of the string, are reflected at the ends, and then return. These pulses return while the hammer is still in contact with the string, and since they are inverted by the reflection, they cause an extra series of compression/decompression cycles for the felt. There is considerable hysteresis during these cycles, much more than might have been expected from the type I result. The overall magnitude of the type II force is also somewhat smaller; the hammer is effectively "softer" under the type II conditions. Since the type II arrangement is the one found in real piano, it is important to use this hammer-force characteristic in modeling.

We have chosen to model our hysteretic type II hammer measurements following the proposal of Stulov [30, 33]. He has suggested the form

$$F_h(y_f(t)) = F_0\left[g(y_f(t)) - \epsilon_0 \int_t^{-\infty} g(y_f(t')) \exp\left(-(t-t')/\tau_0\right) dt'\right]. \tag{2}$$

Here, τ_0 is a characteristic (memory) time scale associated with the felt, ϵ_0 is a measure of the magnitude of the hysteresis, and $y_f(t)$ is the variation of the compression with time. In other words, (2) says that the felt "remembers" its previous compression history over a time of order τ_0, and that the force is reduced according to how much the felt has been compressed during that period. The inherent nonlinearity of the hammer is specified by the function $g(z)$; Stulov took this to be a power law

$$g(z) = z^p. \tag{3}$$

Stulov has compared (2) to measurements with real hammers and reported very good agreement using τ_0, ϵ_0, p, and F_0 as fitting parameters. Our own tests of (2) have not shown such good agreement; we have found that it provides only a qualitative (and in some cases semiquantitative) description of the hysteresis shown in Figure 1 [35]. Nevertheless, it is currently the best mathematical description available for the hysteresis, and we have employed it in our modeling calculations.

Our string calculations are based on the equation of motion [8, 10, 36]

$$\frac{\partial^2 y}{\partial t^2} = c_s^2\left[\frac{\partial^2 y}{\partial x^2} - \epsilon\frac{\partial^4 y}{\partial x^4}\right] - \alpha_1\frac{\partial y}{\partial t} + \alpha_2\frac{\partial^3 y}{\partial t^3}, \tag{4}$$

where $y(x,t)$ is the transverse string displacement at time t and position x along the string. $c_s \equiv \sqrt{\mu/T}$ is the wave speed for an ideal string (with stiffness and damping ignored), with T the tension and μ the mass per unit length of the string. When the parameters ϵ, α_1, and α_2 are zero, this is just the simple wave equation. Equation (4) describes only the polarization mode for which the string displacement is parallel to the initial velocity of the hammer. The other transverse mode and also the longitudinal mode are both ignored; experiments have shown that both of these modes are excited in real piano strings [37, 38, 39], but we will leave them for future modeling work. The term in (4) that is proportional to ϵ arises from the stiffness of the string. It turns out that $c_s\epsilon = r_s^2\sqrt{E_s/\rho_s}$, where r_s, E_s, and ρ_s are the radius, Young's

modulus, and density of the string, respectively, [9, 36]. For typical piano strings, ϵ is of order 10^{-4}, so the stiffness term in (4) is small, but it cannot be neglected as it produces the well-known effect of stretched octaves [36]. Damping is accounted for with the terms involving α_1 and α_2; one of these terms is proportional to the string velocity, while the other is proportional to $\partial^3 y/\partial t^3$. This combination makes the damping dependent on frequency in a manner close to that observed experimentally [8, 10].

Our numerical treatment of the string motion employs a finite difference formulation in which both time t and position x are discretized in units Δt_s and Δx_s [8, 9, 10, 40]. The string displacement is then $y(x,t) \equiv y(i\Delta x_s, n\Delta t_s) \equiv y(i,n)$. If the derivatives in (4) are written in finite difference form, this equation can be rearranged to express the string displacement at each spatial location i at time step $n+1$ in terms of the displacement at previous time steps as described by Chaigne and Askenfelt [8, 10]. The equation of motion (4) does not contain the hammer force. This is included by the addition of a term on the right-hand side proportional to F_h, which acts at the hammer strike point. Since the hammer has a finite width, it is customary to spread this force over a small length of the string [8]. So far as we know, the details of how this force is distributed have never been measured; fortunately our modeling results are not very sensitive to this factor (so long as the effective hammer width is qualitatively reasonable). With this approach to the string calculation, the need for numerical stability together with the desired frequency range require that each string be treated as 50–100 vibrating numerical elements [8, 10].

4. THE SOUNDBOARD

Wood is a complicated material [41]. Soundboards are assembled from wood that is "quarter sawn," which means that two of the principal axes of the elastic constant tensor lie in the plane of the board.

The equation of motion for such a thin orthotropic plate is [11, 22, 23, 42]

$$\rho_b h_b \frac{\partial^2 z}{\partial t^2} = -D_x \frac{\partial^4 z}{\partial x^4} - \left(D_x \nu_y + D_y \nu_x + 4D_{xy}\right) \frac{\partial^4 z}{\partial x^2 \partial y^2} - D_y \frac{\partial^4 z}{\partial y^4} + F_s(x,y) - \beta \frac{\partial z}{\partial t}, \tag{5}$$

where the rigidity factors are

$$D_x = \frac{h_b^3 E_x}{12\left(1-\nu_x \nu_y\right)}, \quad D_y = \frac{h_b^3 E_y}{12\left(1-\nu_x \nu_y\right)}, \quad D_{xy} = \frac{h_b^3 G_{xy}}{12}. \tag{6}$$

Here, our board lies in the $x-y$ plane and z is its displacement. (These x and y directions are, of course, *not* the same as the x and y coordinates used in describing the string motion.) The soundboard coordinates x and y run perpendicular and parallel to the grain of the board. E_x and ν_x are Young's modulus and Poisson's ration for the x direction, and so forth for y, G_{xy} is the shear modulus, h_b is the board thickness and ρ_b is its density. The values of all elastic constants were taken from [41]. In order to model the ribs and bridges, the thickness and rigidity factors are position dependent (since these factors are different at the ribs and bridges than on the "bare" board) as described in [11]. There are also some additional terms that enter the equation of motion (5) at the ends of bridges [11, 17, 18, 43]. $F_s(x,y)$ is the force from the strings on the bridge. This force acts at the appropriate bridge location; it is proportional to the component of the string tension perpendicular to the plane of the board, and is calculated from the string portion of the model. Finally, we include a loss term proportional to the parameter β [11]. The physical origin of this term involves elastic losses within the board. We have not attempted to model this physics according to Newton's laws, but have simply chosen a value of β which yields a quality factor for the soundboard modes which is similar to that observed experimentally [11, 24].[1] Finally, we note that the soundboard "acts back" on the strings, since the bridge moves and the strings are attached to the bridge. Hence, the interaction of strings in a unison group, and also sympathetic string vibrations (with the dampers disengaged from the strings) are included in the model.

For the solution of (5), we again employed a finite difference algorithm. The space dimensions x and y were discretized, both in steps of size Δx_b; this spatial step need not be related to the step size for the string Δx_s. As in our previous work on soundboard modeling [11], we chose $\Delta x_b = 2\,\text{cm}$, since this is just small enough to capture the structure of the board, including the widths of the ribs and bridges. Hence, the board was modeled as $\sim 100 \times 100$ vibrating elements.

The behavior of our numerical soundboard can be judged by calculations of the mechanical impedance, Z, as defined by

$$Z = \frac{F}{v_b}, \tag{7}$$

where F is an applied force and v_b is the resulting soundboard velocity. Here, we assume that F is a harmonic (single frequency) force applied at a point on the bridge and v_b is measured at the same point. Figure 2 shows results calculated from our model [11] for the soundboard from an upright piano. Also shown are measurements for a real upright soundboard (with the same dimensions and bridge positions, etc., as in the model). The agreement is quite acceptable, especially considering that parameters such as the dimensions of the soundboard, the position and thickness of the ribs and bridges, and the elastic constants of the board were taken

[1] In principle, one might expect the soundboard losses to be frequency dependent, as found for the string. At present there is no good experimental data on this question, so we have chosen the simplest possible model with just a single loss term in (5).

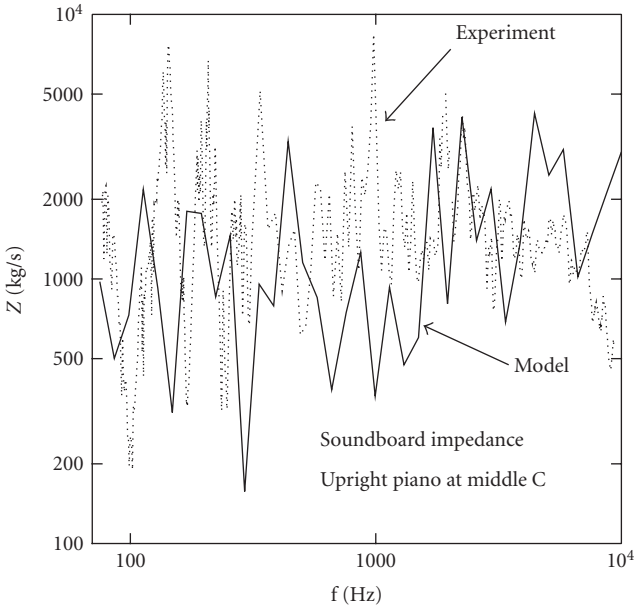

Figure 2: Calculated (solid curve) and measured (dotted curve) mechanical impedance for an upright piano soundboard. Here, the force was applied and the board velocity was measured at the point where the string for middle C crosses the bridge. Results from [11, 24].

from either direct measurements or handbook values (e.g., Young's modulus).

5. THE ROOM

Our time domain room modeling follows the work of Botteldooren [44, 45]. We begin with the usual coupled equations for the velocity and pressure in the room

$$\begin{aligned} \rho_a \frac{\partial v_x}{\partial t} &= -\frac{\partial p}{\partial x}, \\ \rho_a \frac{\partial v_y}{\partial t} &= -\frac{\partial p}{\partial y}, \\ \rho_a \frac{\partial v_z}{\partial t} &= -\frac{\partial p}{\partial z}, \\ \frac{\partial p}{\partial t} &= \rho_a c_a^2 \left[-\frac{\partial v_x}{\partial x} - \frac{\partial v_y}{\partial y} - \frac{\partial v_z}{\partial z} \right], \end{aligned} \tag{8}$$

where p is the pressure, the velocity components are v_x, v_y, and v_z, ρ_a is the density, and c_a is the speed of sound in air. This family of equations is similar in form to an electromagnetic problem, and much is known about how to deal with it numerically. We employ a finite difference approach in which staggered grids in both space and time are used for the pressure and velocity. Given a time step Δt_r, the pressure is computed at times $n\Delta t_r$ while the velocity is computed at times $(n+1/2)\Delta t_r$. A similar staggered grid is used for the space coordinates, with the pressure calculated on the grid $i\Delta x_r$, $j\Delta x_r$, $k\Delta x_r$, while v_x is calculated on the staggered grid $(i+1/2)\Delta x_r$, $j\Delta x_r$, and $k\Delta x_r$. The grids for v_y and v_z are arranged in a similar manner, as explained in [44, 45].

Sound is generated in this numerical room by the vibration of the soundboard. We situate the soundboard from the previous section on a plane perpendicular to the z direction in the room, approximately 1 m from the nearest parallel wall (i.e., the floor). At each time step the velocity v_z of the room air at the surface of the soundboard is set to the calculated soundboard velocity at that instant, as obtained from the soundboard calculation.

The room is taken to be a rectangular box with the same acoustical properties for all 6 walls. The walls of the room are modeled in terms of their acoustic impedance, Z, with

$$p = Z v_n, \tag{9}$$

where v_n is the component of the (air) velocity normal to the wall [46]. Measurements of Z for a number of materials [47] have found that it is typically frequency dependent with the form

$$Z(\omega) \approx Z_0 - \frac{iZ'}{\omega}, \tag{10}$$

where ω is the angular frequency. Incorporating this frequency domain expression for the acoustic impedance into our time domain treatment was done in the manner described in [45].

The time step for the room calculation was $\Delta t_r = 1/22050 \approx 4.5 \times 10^{-4}$ s, as explained in the next section. The choice of spatial step size Δx_r was then influenced by two considerations. First, in order for the finite difference algorithm to be numerically stable in three dimensions, one must have $\Delta x_r/(\sqrt{3}\Delta t_r) > c_a$. Second, it is convenient for the spatial steps for the soundboard and room to be commensurate. In the calculations described below, the room step size was $\Delta x_r = 4$ cm, that is, twice the soundboard step size. When using the calculated soundboard velocity to obtain the room velocity at the soundboard surface, we averaged over 4 soundboard grid points for each room grid point. Typical numerical rooms were $3\times4\times4\,\mathrm{m}^3$, and thus contained $\sim 10^6$ finite difference elements.

Figure 3 shows results for the sound generation by an upright soundboard. Here, the soundboard was driven harmonically at the point where the string for middle C contacts the bridge, and we plot the sound pressure normalized by the board velocity at the driving point [25]. It is seen that the model results compare well with the experiments. This provides a check on both the soundboard and the room models.

6. PUTTING IT ALL TOGETHER

Our model involves several distinct but coupled subsystems—the hammers/strings, the soundboard, and the room—and it is useful to review how they fit together computationally. The calculation begins by giving some initial velocity to a particular hammer. This hammer then strikes a string (or strings), and they interact through either (1) or (2). This sets the string(s) for that note into motion, and these

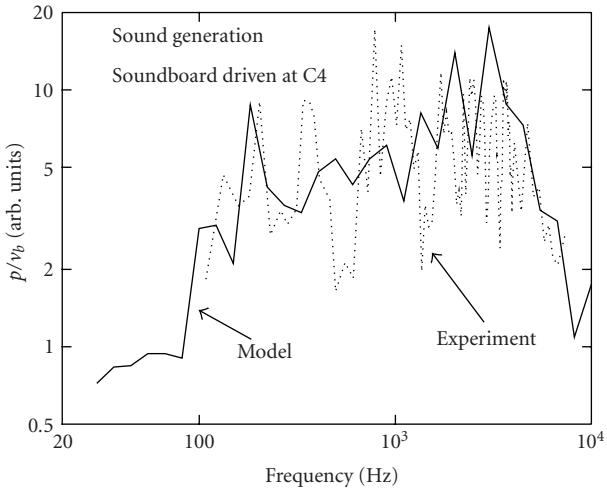

FIGURE 3: Results for the sound pressure normalized by the soundboard velocity for an upright piano soundboard: calculated (solid curve) and measured (dotted curve). The board was driven at the point where the string for middle C crosses the bridge. Results from [25].

in turn act on the bridge and soundboard. As we have already mentioned, the vibrations of each component of our model are calculated with a finite difference algorithm, each with an associated time step. Since the systems are coupled—that is, the strings drive the soundboard, the soundboard acts back on the strings, and the soundboard drives the room—it would be computationally simpler to use the same value of the time step for all three subsystems. However, the equation of motion for the soundboard is highly dispersive, and stability requirements demand a much smaller time step for the soundboard than is needed for string and room simulations. Given the large number of room elements, this would greatly (and unnecessarily) slow down the calculation. We have therefore chosen to instead make the various time steps commensurate, with

$$\begin{aligned} \Delta t_r &= \left(\frac{1}{22050}\right) \text{s}, \\ \Delta t_s &= \frac{\Delta t_r}{4}, \\ \Delta t_b &= \frac{\Delta t_s}{6}, \end{aligned} \tag{11}$$

where the subscripts correspond to the room (r), string (s), and soundboard (b). To explain this hierarchy, we first note that the room time step is chosen to be compatible with common audio hardware and software; $1/\Delta t_r$ is commensurate with the data rates commonly used in CD sound formats. We then see that each room time step contains 4 string time steps; that is, the string algorithm makes 4 iterations for each iteration of the room model. Likewise, each string time step contains 6 soundboard steps.

The overall computational speed is currently somewhat less than "real time." With a typical personal computer (clock speed 1 GHz), a 1 minute simulation requires approximately 30 minutes of computer time. Of course, this gap will narrow in the future in accord with Moore's law. In addition, the model should transfer easily to a cluster (i.e., multi-CPU) machine. We have also explored an alternative approach to the room modeling involving a ray tracing approach [48]. Ray tracing allows one to express the relationship between soundboard velocity and sound pressure as a multiparameter map, involving approximately 10^4 parameters. The values of these parameters can be precalculated and stored, resulting in about an order of magnitude speed-up in the calculation as compared to the room algorithm described above.

7. ANALYSIS OF THE RESULTS: WHAT HAVE WE LEARNED AND WHERE DO WE GO NEXT?

In the previous section, we saw that a real-time Newton's law simulation of the piano is well within reach. While such a simulation would certainly be interesting, it is not a primary goal of our work. We instead wish to use the modeling to learn about the instrument. With that in mind, we now consider the quality of the tones calculated with the current version of the model.

In our initial modeling, we employed power law hammers described by (1) with parameters based on type I hammer experiments by our group [31]. The results were disappointing—it is hard to accurately describe the tones in words, but they sounded distinctly plucked and somewhat metallic. While we cannot include our calculated sounds as part of this paper, they are available on our website http://www.physics.purdue.edu/piano. After many modeling calculations, we came to the conclusion that the hammer model—for example, the power law description (1)—was the problem. Note that we do *not* claim that power law hammers must always give unsatisfactory results. Our point is that when the power law parameters are chosen to fit the type I behavior of real hammers, the calculated tones are poor. It is certainly possible (and indeed, likely) that power law parameters that will yield good piano tones can be found. However, based on our experience, it seems that these parameters should be viewed as fitting parameters, as they may not accurately describe any real hammers.

This led us to the type II hammer experiments described above, and to a description of the hammer-string force in terms of the Stulov function (2), with parameters (τ_0, ϵ_0, etc.) taken from these type II experiments [35]. The results were much improved. While they are not yet "Steinway quality," it is our opinion that the calculated tones could be mistaken for a real piano. In that sense, they pass a sort of acoustical Turing test. Our conclusion is that the hammers are an essential part of the instrument. This is hardly a revolutionary result. However, based on our modeling, we can also make a somewhat stronger statement: in order to obtain a realistic piano tone, the modeling should be based on hammer parameters observed in type II measurements, with the hysteresis included in the model.

There are a number of issues that we plan to address in the future. (1) The hammer portion of the model still

needs attention. Our experiments [35] indicate that while the Stulov function does provide a qualitative description of the hammer force hysteresis, there are significant quantitative differences. It may be necessary to develop a better functional description to replace the Stulov form. (2) As it currently stands, our string model includes only one polarization mode, corresponding to vibrations parallel to the initial hammer velocity. It is well known that the other transverse polarization mode can be important [37]. This can be readily included, but will require a more general soundboard model since the two transverse modes couple through the motion of the bridge. (3) The soundboard of a real piano is supported by a case. Measurements in our laboratory indicate that the case acceleration can be as large as 5% or so of the soundboard acceleration, so the sound emitted by the case is considerable. (4) We plan to refine the room model. Our current room model is certainly a very crude approximation to a realistic room. Real rooms have wall coverings of various types (with differing values of the acoustic impedances), and contain chairs and other objects. At our current level of sophistication, it appears that the hammers are more of a limitation than the room model, but this may well change as the hammer modeling is improved.

In conclusion, we have made good progress in developing a physical model of the piano. It is now possible to produce realistic tones using Newton's laws with realistic and independently determined instrument parameters. Further improvements of the model seem quite feasible. We believe that physical modeling can provide new insights into the piano, and that similar approaches can be applied to other instruments.

ACKNOWLEDGMENTS

We thank P. Muzikar, T. Rossing, A. Tubis, and G. Weinreich for many helpful and critical discussions. We also are indebted to A. Korty, J. Winans II, J. Millis, S. Dietz, J. Jourdan, J. Roberts, and L. Reuff for their contributions to our piano studies. This work was supported by National Science Foundation (NSF) through Grant PHY-9988562.

REFERENCES

[1] D. E. Hall, "Piano string excitation in the case of small hammer mass," *Journal of the Acoustical Society of America*, vol. 79, no. 1, pp. 141–147, 1986.

[2] D. E. Hall, "Piano string excitation II: General solution for a hard narrow hammer," *Journal of the Acoustical Society of America*, vol. 81, no. 2, pp. 535–546, 1987.

[3] D. E. Hall, "Piano string excitation III: General solution for a soft narrow hammer," *Journal of the Acoustical Society of America*, vol. 81, no. 2, pp. 547–555, 1987.

[4] D. E. Hall and A. Askenfelt, "Piano string excitation V: Spectra for real hammers and strings," *Journal of the Acoustical Society of America*, vol. 83, no. 4, pp. 1627–1638, 1988.

[5] D. E. Hall, "Piano string excitation. VI: Nonlinear modeling," *Journal of the Acoustical Society of America*, vol. 92, no. 1, pp. 95–105, 1992.

[6] H. Suzuki, "Model analysis of a hammer-string interaction," *Journal of the Acoustical Society of America*, vol. 82, no. 4, pp. 1145–1151, 1987.

[7] X. Boutillon, "Model for piano hammers: Experimental determination and digital simulation," *Journal of the Acoustical Society of America*, vol. 83, no. 2, pp. 746–754, 1988.

[8] A. Chaigne and A. Askenfelt, "Numerical simulations of piano strings. I. A physical model for a struck string using finite difference method," *Journal of the Acoustical Society of America*, vol. 95, no. 2, pp. 1112–1118, 1994.

[9] A. Chaigne and A. Askenfelt, "Numerical simulations of piano strings. II. Comparisons with measurements and systematic exploration of some hammer-string parameters," *Journal of the Acoustical Society of America*, vol. 95, no. 3, pp. 1631–1640, 1994.

[10] A. Chaigne, "On the use of finite differences for musical synthesis. Application to plucked stringed instruments," *Journal d'Acoustique*, vol. 5, no. 2, pp. 181–211, 1992.

[11] N. Giordano, "Simple model of a piano soundboard," *Journal of the Acoustical Society of America*, vol. 102, no. 2, pp. 1159–1168, 1997.

[12] H. A. Conklin Jr., "Design and tone in the mechanoacoustic piano. Part I. Piano hammers and tonal effects," *Journal of the Acoustical Society of America*, vol. 99, no. 6, pp. 3286–3296, 1996.

[13] H. Suzuki and I. Nakamura, "Acoustics of pianos," *Appl. Acoustics*, vol. 30, pp. 147–205, 1990.

[14] H. A. Conklin Jr., "Design and tone in the mechanoacoustic piano. Part II. Piano structure," *Journal of the Acoustical Society of America*, vol. 100, no. 2, pp. 695–708, 1996.

[15] H. A. Conklin Jr., "Design and tone in the mechanoacoustic piano. Part III. Piano strings and scale design," *Journal of the Acoustical Society of America*, vol. 100, no. 3, pp. 1286–1298, 1996.

[16] B. E. Richardson, G. P. Walker, and M. Brooke, "Synthesis of guitar tones from fundamental parameters relating to construction," *Proceedings of the Institute of Acoustics*, vol. 12, no. 1, pp. 757–764, 1990.

[17] A. Chaigne and V. Doutaut, "Numerical simulations of xylophones. I. Time-domain modeling of the vibrating bars," *Journal of the Acoustical Society of America*, vol. 101, no. 1, pp. 539–557, 1997.

[18] V. Doutaut, D. Matignon, and A. Chaigne, "Numerical simulations of xylophones. II. Time-domain modeling of the resonator and of the radiated sound pressure," *Journal of the Acoustical Society of America*, vol. 104, no. 3, pp. 1633–1647, 1998.

[19] L. Rhaouti, A. Chaigne, and P. Joly, "Time-domain modeling and numerical simulation of a kettledrum," *Journal of the Acoustical Society of America*, vol. 105, no. 6, pp. 3545–3562, 1999.

[20] B. Bank, F. Avanzini, G. Borin, G. De Poli, F. Fontana, and D. Rocchesso, "Physically informed signal processing methods for piano sound synthesis: a research overview," *EURASIP Journal on Applied Signal Processing*, vol. 2003, no. 10, pp. 941–952, 2003.

[21] N. Giordano, M. Jiang, and S. Dietz, "Experimental and computational studies of the piano," in *Proc. 17th International Congress on Acoustics*, vol. 4, Rome, Italy, September 2001.

[22] J. Kindel and I.-C. Wang, "Modal analysis and finite element analysis of a piano soundboard," in *Proc. 5th International Modal Analysis Conference*, pp. 1545–1549, Union College, Schenectady, NY, USA, 1987.

[23] J. Kindel, "Modal analysis and finite element analysis of a piano soundboard," M.S. thesis, University of Cincinnati, Cincinnati, Ohio, USA, 1989.

[24] N. Giordano, "Mechanical impedance of a piano soundboard," *Journal of the Acoustical Society of America*, vol. 103, no. 4, pp. 2128–2133, 1998.
[25] N. Giordano, "Sound production by a vibrating piano soundboard: Experiment," *Journal of the Acoustical Society of America*, vol. 104, no. 3, pp. 1648–1653, 1998.
[26] A. Askenfelt and E. V. Jansson, "From touch to string vibrations. II. The motion of the key and hammer," *Journal of the Acoustical Society of America*, vol. 90, no. 5, pp. 2383–2393, 1991.
[27] T. Yanagisawa, K. Nakamura, and H. Aiko, "Experimental study on force-time curve during the contact between hammer and piano string," *Journal of the Acoustical Society of Japan*, vol. 37, pp. 627–633, 1981.
[28] T. Yanagisawa and K. Nakamura, "Dynamic compression characteristics of piano hammer," *Transactions of Musical Acoustics Technical Group Meeting of the Acoustic Society of Japan*, vol. 1, pp. 14–17, 1982.
[29] T. Yanagisawa and K. Nakamura, "Dynamic compression characteristics of piano hammer felt," *Journal of the Acoustical Society of Japan*, vol. 40, pp. 725–729, 1984.
[30] A. Stulov, "Hysteretic model of the grand piano hammer felt," *Journal of the Acoustical Society of America*, vol. 97, no. 4, pp. 2577–2585, 1995.
[31] N. Giordano and J. P. Winans II, "Piano hammers and their force compression characteristics: does a power law make sense?," *Journal of the Acoustical Society of America*, vol. 107, no. 4, pp. 2248–2255, 2000.
[32] N. Giordano and J. P. Millis, "Hysteretic behavior of piano hammers," in *Proc. International Symposium on Musical Acoustics*, D. Bonsi, D. Gonzalez, and D. Stanzial, Eds., pp. 237–240, Perugia, Umbria, Italy, September 2001.
[33] A. Stulov and A. Mägi, "Piano hammer: Theory and experiment," in *Proc. International Symposium on Musical Acoustics*, D. Bonsi, D. Gonzalez, and D. Stanzial, Eds., pp. 215–220, Perugia, Umbria, Italy, September 2001.
[34] J. I. Dunlop, "Nonlinear vibration properties of felt pads," *Journal of the Acoustical Society of America*, vol. 88, no. 2, pp. 911–917, 1990.
[35] N. Giordano and J. P. Millis, "Using physical modeling to learn about the piano: New insights into the hammer-string force," in *Proc. International Congress on Acoustics*, S. Furui, H. Kanai, and Y. Iwaya, Eds., pp. III–2113, Kyoto, Japan, April 2004.
[36] N. H. Fletcher and T. D. Rossing, *The Physics of Musical Instruments*, Springer-Verlag, New York, NY, USA, 1991.
[37] G. Weinreich, "Coupled piano strings," *Journal of the Acoustical Society of America*, vol. 62, no. 6, pp. 1474–1484, 1977.
[38] M. Podlesak and A. R. Lee, "Dispersion of waves in piano strings," *Journal of the Acoustical Society of America*, vol. 83, no. 1, pp. 305–317, 1988.
[39] N. Giordano and A. J. Korty, "Motion of a piano string: longitudinal vibrations and the role of the bridge," *Journal of the Acoustical Society of America*, vol. 100, no. 6, pp. 3899–3908, 1996.
[40] N. Giordano, *Computational Physics*, Prentice-Hall, Upper Saddle River, NJ, USA, 1997.
[41] V. Bucur, *Acoustics of Wood*, CRC Press, Boca Raton, Fla, USA, 1995.
[42] S. G. Lekhnitskii, *Anisotropic Plates*, Gordon and Breach Science Publishers, New York, NY, USA, 1968.
[43] J. W. S. Rayleigh, *Theory of Sound*, Dover, New York, NY, USA, 1945.
[44] D. Botteldooren, "Acoustical finite-difference time-domain simulation in a quasi-Cartesian grid," *Journal of the Acoustical Society of America*, vol. 95, no. 5, pp. 2313–2319, 1994.
[45] D. Botteldooren, "Finite-difference time-domain simulation of low-frequency room acoustic problems," *Journal of the Acoustical Society of America*, vol. 98, no. 6, pp. 3302–3308, 1995.
[46] P. M. Morse and K. U. Ingard, *Theoretical Acoustics*, Princeton University Press, Princeton, NJ, USA, 1986.
[47] L. L. Beranek, "Acoustic impedance of commercial materials and the performance of rectangular rooms with one treated surface," *Journal of the Acoustical Society of America*, vol. 12, pp. 14–23, 1940.
[48] M. Jiang, "Room acoustics and physical modeling of the piano," M.S. thesis, Purdue University, West Lafayette, Ind, USA, 1999.

N. Giordano obtained his Ph.D. from Yale University in 1977, and has been at the Department of Physics at Purdue University since 1979. His research interests include mesoscopic and nanoscale physics, computational physics, and musical acoustics. He is the author of the textbook *Computational Physics* (Prentice-Hall, 1997). He also collects and restores antique pianos.

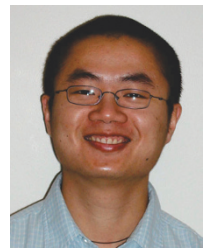

M. Jiang has a B.S. degree in physics (1997) from Peking University, China, and M.S. degrees in both physics and computer science (1999) from Purdue University. Some of the work described in this paper was part of his physics M.S. thesis. After graduation, he worked as a software engineer for two years, developing Unix kernel software and device drivers. In 2002, he moved to Bozeman, Montana, where he is now pursuing a Ph.D. in computer science in Montana State University. Minghui's current research interests include the design of algorithms, computational geometry, and biological modeling and bioinformatics.